Advances in Nonlinear Variational Inequalities
ISSN: 1092-910X
Vol 27 No. 4(2024)

Dimensionality Reduction of Hyperspectral Images Using Pixel Block Distance for Efficient Classification

Amit R Pathare[1], Atul S Joshi[2], Nitin S Thakare[3], Parag P Gudadhe[4]

[1,3,4] Assistant Professor, Department of Electronics & Telecommunication Engineering, PRMIT&R, Amravati, India
[2] Professor, Department of Electronics & Telecommunication Engineering, Sipna COET, Amravti, India
[1]pathare.amit2909@gmail.com (corresponding author)
[2]atuljoshi1974@rediffmail.com, [3]nit.thakare12@gmail.com, [4]ppgudadhe@mitra.ac.in

Article History:

Received: *11-03-2024*

Revised: *06-05-2024*

Accepted: *30-05-2024*

Abstract:
Hyperspectral imaging provides useful information in the field of satellite imaging. The extensive spectral and spatial data contained within hyperspectral images (HSI) needs to be analyzed for retrieving the insights about the geographical details. The redundancy in spectral bands results in high dimensionality. The high dimensionality of HSI results in increased computational complexity. This subsequently influences the classification accuracy. Consequently, dimensionality reduction (DR) of HSI is essential before the classification. State-of-the-art DR techniques fail to recognize the nonlinearity in hyperspectral data. The proposed distance measure utilizes information derived from both spatial and spectral domains. The existing DR methods can be included with the proposed distance measure to address the issue of nonlinearity in HSI data. The tests are carried out on DR methods included with the proposed distance measure to assess the results of classification utilizing Support Vector Machine (SVM). Results of classification show that DR techniques incorporated with proposed measures address the nonlinearity present in HSI data.

Keywords: Hyperspectral Image (HSI), Dimensionality reduction (DR), Pixel Block Distance (PBD), weighted neighbourhood matrix.

1. Introduction

The advancement of image sensors has made hyperspectral imaging (HSI) one of the most trusted techniques for a variety of applications, like land cover mapping, precision agriculture, vegetation monitoring, and military applications [1]. Sophisticated observations at hundreds of linked, ultra-thin spectral bands are provided via a HSI data cube, including one spectral and two spatial dimensions. Hyperspectral image structure is illustrated in Fig. 1.

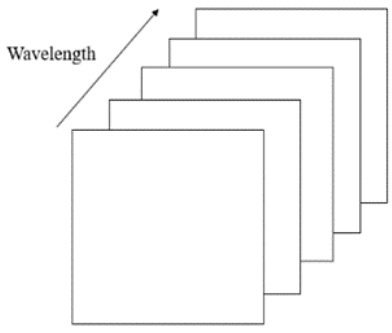

Fig. 1. A HSI is an array of 2-D images captured at various wavelengths.

The Hyperspectral Imaging (HSI) system possesses extensive and valuable spectral and spatial data, enhancing the ability to differentiate between various objects and is beneficial for a broad range of applications like agriculture, chemistry, physics, environment, earth science, oceanography, and surveillance [2]. The narrowly placed bands have high redundancy among pixels. The spatial and spectral domains contain redundancy, which results in the Hughes phenomenon, often referred to as the curse of high dimensionality [3]. The high dimensionality causes complexity in feature space, which has a greater influence on the classification accuracy. Therefore, it is necessary to address the issue of redundancy. Dimensionality reduction (DR) is a technique that is used prior to classification that reduces the redundancy and complexity of feature space while the important, descriptive features of hyperspectral data are retained for the efficient classification [4]. Dimensionality reduction improves classification accuracy and time required for classification. In general, the DR approach converts HSI into a smaller and more comprehensible representation by reducing their dimensionality [5]. Optimally, the decreased dimensionality refers to the minimal feature required to accurately represent the data with minimum loss [4].

As per the literature, DR techniques on hyperspectral images can be broadly classified into linear and nonlinear methods [6]. Principal Component Analysis (PCA) assumes that the consecutive bands in a HSI exhibit strong correlation and redundancy. PCA utilizes Euclidean distance (ED) as the metric for measuring spatial similarity [7]. A constraint of linear techniques is their inability to recognize the curved and nonlinear characteristics of the input data. The nonlinearity in hyperspectral data is caused by the existence of a variable attenuating medium in the scene, multipath scatter among subpixel components, and nonlinear oscillations in reflectance. Additionally, HSI exhibits increased nonlinearity as a result of the high spectral resolution of sensors [6]. Nonlinearity has an impact on the outcome of the classification. Hence, it is imperative to tackle the nonlinearity in HSI data while aiming to achieve dimensionality reduction.

Nonlinear methods focus on creating the coordinate system that lies on the data manifold [8]. Nonlinear methods first construct a neighborhood graph using ED as a spatial similarity measure, followed by assigning the weights to the neighborhood graph using various approaches. The Isometric Feature Mapping (ISOMAP) method utilizes the pairwise geodesic distance over the data manifold to give weights, whereas Locally Linear Embedding (LLE) uses the nearest neighbors in the feature space to create a linear coefficient combination [9]. Nonlinear methods increase computational complexity due to coordinate calculation along the manifold. A method like ISOMAP has the disadvantage of short circuiting, which arises due to the closely spaced data manifold [6], [10]. While assigning the weights to neighborhood graphs, ISOMAP may cause memory exhaustion due to the vast size of HSI data.

Nevertheless, the linear and nonlinear DR approaches treat each pixel individually, disregarding any hint of commonalities in physical qualities. The spatial correlation of pixels in images is a well-established phenomenon, meaning that they are connected to each other in terms of their position [11]. This spatial relationship allows us to extract important information from the spatial domain of the image. Regarding the classification of HSI data, it is common for the pixels in a small vicinity to be assigned the same class designation. Hence, it is necessary to utilize the spatial domain of the HSI data [12].

In this paper, a measure that includes both spatial and spectral information to exploit the relationship between observing pixels. The proposed pixel block distance (PBD) measure uses the pixels and their spatial neighbors to measure the block-wise pixel correlation. The PBD measure can be utilized in conventional linear and nonlinear methods to address the issue of nonlinearity in HSI data cube.

2. METHODOLOGY

The typical PCA and LLE methods are discussed first, followed by the proposed PBD measure.

2.1 Principal Component Analysis (PCA):

For given HSI data set $H = (H_1, H_2, H_3, \dots\dots, H_b)$ where b is the number of spectral bands. Each spectral band has a spatial resolution of $r \times c$. PCA converts high dimensional H data set into low dimensional subspace while conserving the covariance of original data.

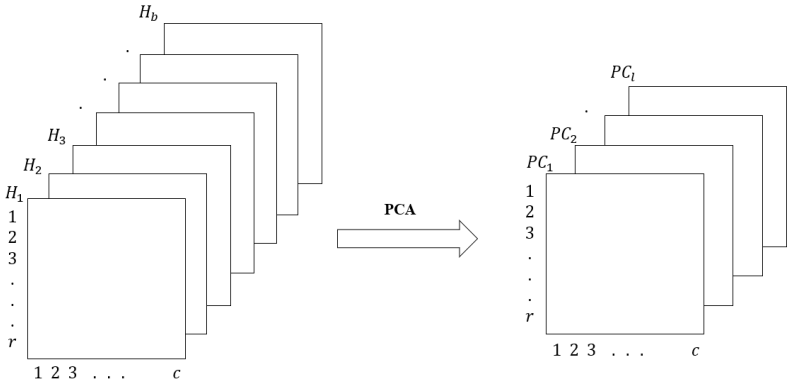

Fig. 2. Dimensionality reduction using PCA, $b >> l$

First, rearrange the HSI data into $rc \times b$ data matrix.

$$H_n = [H_{1n};\ H_{2n}; H_{3n}; \dots;\ H_{bn}]^T \tag{1}$$

where n varies from 1 to rc.

Mean spectral vector is calculated as below.

$$I = H - \bar{I} \tag{2}$$

$$\bar{I} = \frac{1}{rc}\sum_{n=1}^{rc} H_n \tag{3}$$

Covariance matrix is given as,

$$cv = E\{I\ I^T\} \tag{4}$$

Get eigen values and vector by decomposing covariance matrix,

$$cv = ODO^T \tag{5}$$

where O is orthonormal matrix formed using eigen vectors. D is diagonal matrix formed using eigen values of cv.

$$D = [\lambda_1, \lambda_2, \lambda_3, \dots, \lambda_n] \tag{6}$$

where $\lambda_1, \lambda_2, \lambda_3, \dots, \lambda_n$ are the eigen values of covariance matrix cv.

Eigen vectors $v_1, v_2, v_3, \dots, v_n$ of covariance matrix cv forms orthonormal matrix O.

$$O = [v_1, v_2, v_3, \dots, v_n] \tag{7}$$

First l eigen vectors may be used for transforming the HSI data into reduced data ($l << b$).

The transformation expressed linearly as,

$$y_n = O^T H_n \tag{8}$$

Data projection results in,

$$PC = reduced(y_n) = [PC_{n1};\ PC_{n2}; PC_{n3};\ \dots;\ PC_{nl}]^T \tag{9}$$

2.2 Locally Linear Embedding (LLE) algorithm:

LLE is a nonlinear DR method that assumes that data is very large and noise-free. It considers that any small region in data is locally linear and every vector can be reconstituted in terms of its neighbors [12]. For given HSI data set $H = (H_1,\ H_2, H_3, \dots\dots, H_b)$ where b is number of spectral bands, each band has spatial resolution of $r \times c$, construct the graph $Gh(Nd, E, W)$ by identifying the index set of nearest neighbours $\phi(i)$ for each pixel $H_i(r, c)$ as node Nd_i of the graph. E is edge of the graph that connects the nodes Nd of neighboring data points. W is weight assigned to edges using the least square method as,

Minimize,

$$\sum_{i=1}^{b} \left\| H_i - \sum_{j \in \emptyset(i)} W_{i,j} H_j \right\|$$

$$subject\ to\ \ W_{i,j} = 0, for\ j \notin \phi(i), \qquad \sum_{j \in \emptyset(i)} W_{i,j} = 1 \tag{10}$$

After obtaining the weights, the next phase involves solving another least square problem to transfer each high-dimensional observed pixel into low-dimensional feature space.

Minimize,

$$\sum_{i=1}^{b} \left\| y_i - \sum_{j \in \emptyset(i)} W_{i,j} y_j \right\|$$

$$subject\ to\ \ \sum_i y_i = 0, \qquad \frac{1}{b} \sum_i y_i {y_i}^T = I \tag{11}$$

where $Y = (y_1, y_2, y_3, \dots, y_l)$ is the reduced dimensionality of original HSI data. LLE preserve the local structure of data.

2.3 Pixel-block-distance (PBD):

As defined earlier, H is an HSI data cube having l number of bands, and each band has $r \times c$ pixels. Assume that H_{pq} is pixel at the discrete spatial coordinates (p, q) and $n = r \times c$ is number pixels. In

HSI data, pixels that belong to a local neighborhood fit into the same class, which represents the same object material. Such pixels have highly correlated spectral characteristics.

A local neighborhood of $w \times w$ odd window size with H_{pq} at center can be defined as,

$$\psi(H_{pq}) = \left\{H_{ef} : e = p - \left(\frac{w-1}{2}\right), \dots, p, \dots, p + \left(\frac{w-1}{2}\right); f = q - \left(\frac{w-1}{2}\right), \dots, q, \dots, q + \left(\frac{w-1}{2}\right)\right\} \tag{12}$$

A local neighborhood of 3×3 with H_{pq} at centre is illustrated in Fig. 3

$H_{p-1,q-1}$	$H_{p-1,q}$	$H_{p-1,q+1}$
$H_{p,q-1}$	$H_{p,q}$	$H_{p,q+1}$
$H_{p+1,q-1}$	$H_{p+1,q}$	$H_{p+1,q+1}$

Fig. 3. Local neighbourhood of 3×3 with H_{pq} at centre

Assume that α_k and β_k be the k^{th} element of neighbourhood $\psi(H_{pq})$ and $\psi(H_{st})$.

$$\psi(H_{pq}) = \{\alpha_1, \alpha_2, \alpha_3, \dots, \alpha_{w\times w}\} \tag{13}$$

$$\psi(H_{st}) = \{\beta_1, \beta_2, \beta_3, \dots, \beta_{w\times w}\} \tag{14}$$

The proposed pixel block distance (PBD) between the pixels, H_{pq} and H_{st} is defined as

$$d_{PBD}(H_{pq}, H_{st}) = \sum_{k=1}^{w\times w} d_u(\alpha_k, \beta_k)$$

where $d_u(\alpha_k, \beta_k)$ is undirected distance between two pixels α_k and β_k and is given as,

$$d_u(\alpha_k, \beta_k) = \max\left(\min_{\beta\in H_{st}} d(\alpha_k, \beta), \min_{\alpha\in H_{pq}} d(\beta_k, \alpha)\right) \tag{16}$$

Hence Equation (15) becomes,

$$d_{PBD}(H_{pq}, H_{st}) = \sum_{k=1}^{w\times w} \left\{\max\left(\min_{\beta\in H_{st}} d(\alpha_k, \beta), \min_{\alpha\in H_{pq}} d(\beta_k, \alpha)\right)\right\} \tag{17}$$

The computation of PBD for the neighborhood of 3×3 is depicted in Fig. 4. PBD describes the distance between two pixels H_{pq} and H_{st} which best describes the measure between pixels and its neighborhood.

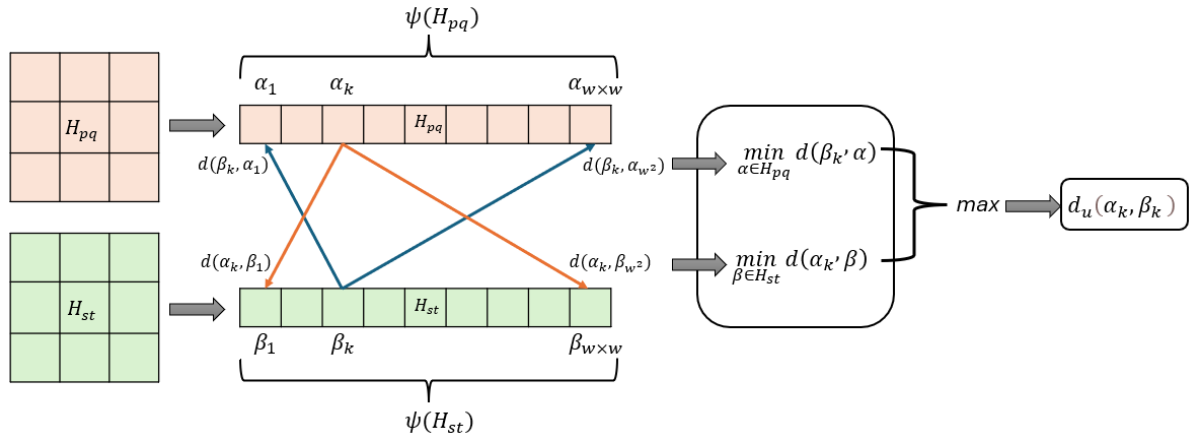

Fig. 4. PBD with neighbourhood of 3 × 3

The size of the neighborhood of pixels under consideration for PBD should be optimal. If the window size is too small, then spatial information in the neighborhood is weak, whereas if the window size is too large, then unwanted, uncorrelated information may get included, which results in complexity.

2.4 DR based on PBD:

Traditional linear and nonlinear DR methods like PCA [13] and LLE [6] can be incorporated with PBD, due to which spatial information can be retained while reducing dimensionality. In the PCA method, instead of ED, PBD may be used while calculating Eigen values and Eigen vectors of the covariance matrix in equation (4). High-dimensional HSI data is then projected into reduced dimensionality using equations (8) and (9).

Algorithm: Dimensionality reduction using PCA incorporated with PBD
Input: Hyperspectral image H with b bands, each band having spatial resolution of $r \times c$
Step1: HSI data $H = (H_1, H_2, H_3, \dots\dots, H_b)$ is rearranged to form data matrix H_n Step2: Compute Mean spectral vector I using H and H_n Step3: Covariance matrix is constructed using the proposed distance measure PBD. Step4: Eigen vectors are derived by performing Eigen decomposition of covariance matrix. Step5: Top l eigen vectors ($l << b$) are used to form orthonormal matrix Step6: Multiplication between orthonormal matrix and HSI data matrix yields reduced dimensionality
Output: Reduced number of l principal components, $l << b$

LLE method of DR discussed earlier, in that PBD can be used to construct the neighborhood graph from HSI feature space. Construct the neighbourhood graph using the pixel black distance d_{PBD} between the group of pixels in input HSI data. The weight to the edges of the graph Gh is assigned using the least square problem in equation(10).

Algorithm: Dimensionality reduction using nonlinear approach, LLE included with PBD
Input: Hyperspectral image $H_n = [H_{1n};\ H_{2n}; H_{3n}; \dots;\ H_{bn}]^T$ with b bands, each band having spatial resolution of $r \times c$
Step1: Form data matrix H_n using HSI data $H = (H_1,\ H_2, H_3, \dots \dots, H_b) \in R^{b \times n}$ Step2: Compute the nearest neighbouring matrix $\phi(i)$ for each pixel $H_i(r, c)$ Step3: Distance matrix D_{PBD} between pixels of neighborhood Step4: Weighted graph $Gh(Nd, E, W_{PBD})$ where weight W_{PBD} of edge E is assigned by solving least square method in equation (10) Step5: Transfer the data into lower dimensional space by solving least square problem in (11)
Output: Reduced dimensionality $Y = (y_1, y_2, y_3, \dots, y_l)$ where $l << b$

3. Experiment & Result:

A hyperspectral image of Indian Pines is used for experimental purposes. Indian Pine HSI has 220 spectral bands with a resolution of 145 x 145. This image is captured by an AVRIS sensor $0.4\ \mu m\ to\ 2.5\ \mu m$ wavelength. A false colour image of an Indian Pine HSI cube and its groundtruth image having 16 classes is shown in Fig. 5. Table I demonstrates the number of samples, i.e., the number of pixels in each class of groundtruth image. The groundtruth image data is useful in validating the accuracy of the result of dimensionality reduction and classification [14]. Some of the bands in the database are due to water absorption and clouds, and it doesn't hold any information. So, bands 104-108, 150-163, and 220 are removed before the preprocessing. High-frequency noise from each band is then removed by applying a Gaussian filter.

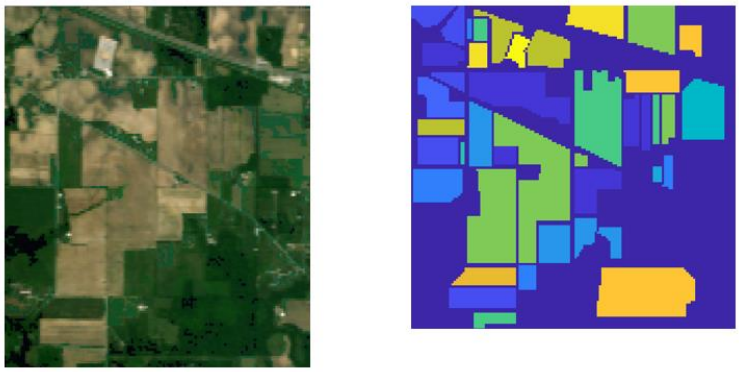

Fig. 5. (a) False color Indian Pines image (b) Ground-truth image having 16 classes

In the experiments, first conventional methods like PCA and LLE with ED [15] as a measure are used for DR, followed by the classification using SVM. In second, the proposed PBD measure is incorporated in the PCA and LLE for DR. Results after classification are compared for the performance of the proposed DR based on a spectral-spatial feature extraction approach.

The classification result is utilized to evaluate the efficacy of the proposed approach. SVM is a supervised classification method [16], [17] that involves training and a test phase. In the experiment, a certain percentage of total pixels from the groundtruth image is used as training pixels, and the remaining pixels are used as test pixels. This ratio is expressed in percentage and called the training-

to-test ratio (TTR). In the experiment, TTR is kept at 10%. The number of pixels from each class used for testing and training is illustrated in Table I. The classification performance is calculated in terms of overall accuracy (OA).

Table I: Total number of pixels, training pixel, and test pixels in each class of Indian Pines groundtruth image (with TTR = 10%)

Sr. No.	Class	Sample (No. of pixels per class)		
		Training	Test	Total
1	Alfalfa	5	41	46
2	Corn-notill	143	1285	1428
3	Corn-mintill	83	747	830
4	Corn	24	213	237
5	Grass-pasture	48	435	483
6	Grass-trees	73	657	730
7	Grass-pasture-mowed	3	25	28
8	Hay-windrowed	48	430	478
9	Oats	2	18	20
10	Soybean-notill	97	875	972
11	Soybean-mintill	246	2210	2455
12	Soybean-clean	59	534	593
13	Wheat	21	185	205
14	Woods	127	1139	1265
15	Buildings-Grass-Trees-Drives	39	347	386
16	Stone-Steel-Towers	9	84	93

On the HSI data having 220 bands, PCA with ED measure is applied for DR. The value of the number of reduced planes is selected over a range of 3 to 30 planes, as shown in Table II. For each DR plane, the classification results are obtained, and the accuracy of the classification is calculated in terms of overall accuracy (OA). The same approach is repeated for the nonlinear DR method, LLE. The weighted graph is constructed, and weights are calculated using ED measure. The reduced dimensionality feature space is classified using a SVM classifier for different numbers of DR planes. The result for both PCA and LLE is given in Table II. The proposed PBD distance measure is incorporated in PCA and LLE. It is then applied to HSI data for the purpose of DR. PBD embedded PCA and LLE is computed by selecting the different window size $w \times w$ of neighborhood for $\psi(H_{st})$ and $\psi(H_{pq})$. Table II shows the results for neighborhoods of 3×3, 5×5, 7×7.

Table II. OA after classification of DR HSI using conventional and methods included with proposed distance measure (TTR=10%, window size=3, 5, 7)

DR method	Euclidean Distance measure		Window size	PBD measure		Window size	PBD measure		Window size	PBD measure	
	PCA	LLE	w x w	PCA	LLE	w x w	PCA	LLE	w x w	PCA	LLE
DR planes	OA %	OA %	3 x 3	OA %	OA %	5 x 5	OA %	OA %	7 x 7	OA %	OA %
3	52.5	53.95		54.64	**55.09**		56.79	**57.14**		57.42	**58.26**
5	64.41	65.96		66.78	**67.29**		68.19	**69.44**		69.37	**70.13**
10	76.83	78.13		78.82	**79.51**		80.21	**81.27**		81.34	**82.73**
15	84.53	83.68		84.14	**84.48**		86.39	**86.51**		87.71	**87.86**
20	88.47	89.17		89.26	**90.07**		91.19	**91.94**		**92.52**	92.49
25	90.23	91.29		91.98	**92.87**		93.06	**94.16**		94.32	**95.47**
30	91.37	92.86		93.66	**93.82**		94.61	**94.98**		95.29	**95.87**

Table III. OA after classification of DR HSI using conventional and methods included with proposed distance measure (TTR=10%, window size=9, 11, 13).

DR method	Window size	PBD measure		Window size	PBD measure		Window size	PBD measure	
	w x w	PCA	LLE	w x w	PCA	LLE	w x w	PCA	LLE
DR planes	9 x 9	OA %	OA %	11 x 11	OA %	OA %	13 x 13	OA %	OA %
3		58.22	**59.67**		**57.88**	57.48		56.23	**56.88**
5		69.81	**71.36**		68.78	**70.57**		67.19	**68.6**
10		81.67	**83.42**		80.89	**82.69**		79.46	**81.43**
15		88.84	**89.13**		87.67	**88.34**		86.73	**87.03**
20		92.86	**93.31**		91.74	**92.67**		90.39	**91.27**
25		95.02	**96.04**		93.93	**94.22**		92.41	**92.69**
30		95.63	**96.31**		94.77	**95.09**		93.89	**94.17**

In Table II and Table III, the overall accuracy of classification for PCA and LLE incorporated with the proposed PBD is shown for different window sizes. Results are compared with conventional ED implemented PCA and LLE. Also, results are computed for several reduced-dimensional planes. It can be observed that the proposed PBD measure improves the OA of classification as compared to the ED measure in PCA and LLE. Fig. 6 shows the OA of classification after the DR of HSI data using PCA. It is seen that OA improves if the proposed PBD distance measure is included in PCA instead of ED. Similarly, the same trend can be observed in Fig. 7, where LLE is used as DR, which is implemented with ED and PBD distance measures.

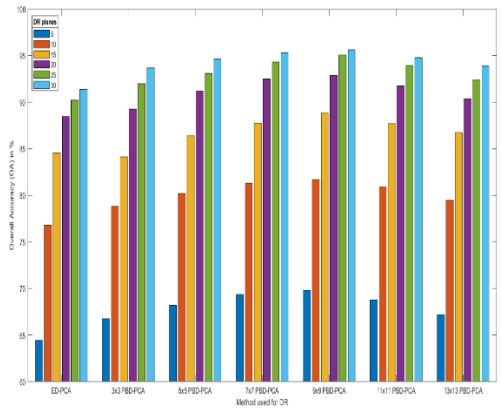

Fig 6: Overall accuracy (OA) curves for several distance measures implemented PCA as DR methods

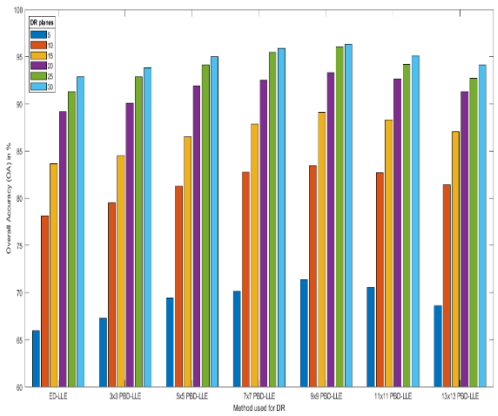

Fig 7: Overall accuracy (OA) curves for several distance measures implemented LLE as DR methods

In PBD measure, the size of the spatial window for a neighborhood of pixels plays an important role in DR techniques. Fig. 8 shows the OA versus distance measure for the reduced dimensionality of 10 planes. It can be observed that as the size of window in PBD increases, more specifically OA for sizes 3, 5, 7, and 9 increases, but for window sizes 11, 13, OA decreases for a particular value of the DR plane. For large values of window size, redundancy in the neighborhood increases, which in turn increases complexity and hence results in decreased OA. On the other hand, if the window size is too small, there is a possibility of losing the trivial relationship between pixels. So, the window size value should be optimally chosen. In the experiment, maximum OA is achieved for 9×9 window size. The size of window depends on the spatial resolution of HSI data, i.e., images having high spatial resolution; the size of window can be of higher order.

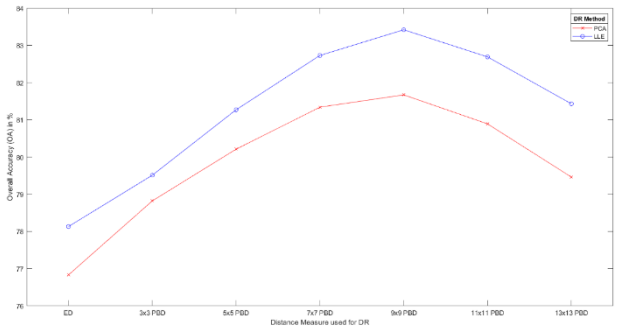

Fig 8: Distance measures vs Overall accuracy (OA) curves for 10 DR planes

4. CONCLUSION

The new distance measure is introduced for dimensionality reduction of hyperspectral images. The introduced measure overcomes the nonlinearity present in the feature space by preserving the local relationship among the pixels from the same class in the data manifold. The proposed PBD measure can be incorporated in both linear and nonlinear DR methods to improve the performance. The proposed distance measure may be the new norm to decide the neighborhood or assigning the weights

in a weighted neighborhood graph in DR methods. The results of the experiments show that DR based on the proposed measure can give better results in terms of OA of classification as compared to usual DR methods in hyperspectral image classification. There is future scope in areas like reducing the computational complexity associated with DR methods like ISOMAP. Furthermore, the criterion for neighborhood window size selection should be investigated for high spatial resolution images.

References

[1] P. Geladi and H. F. Grahn, "Multivariate Image Analysis," *Encyclopedia of Analytical Chemistry,* John Wiley & Sons Ltd.

[2] J. M. Prats-Montalbán, A. de Juan, and A. Ferrer, "Multivariate image analysis: A review with applications," May 2011. doi: 10.1016/j.chemolab.2011.03.002.

[3] D. J. Finney, "Dimensions of Statistics," *Journal of the Royal Statistical Society. Series C (Applied Statistics)*, Vol. 26, No. 3 (1977), pp. 285-289, 1977.

[4] M. Hasanlou and F. Samadzadegan, "Comparative study of intrinsic dimensionality estimation and dimension reduction techniques on hyperspectral images using K-NN classifier," *IEEE Geoscience and Remote Sensing Letters*, vol. 9, no. 6, pp. 1046–1050, 2012, doi: 10.1109/LGRS.2012.2189547.

[5] P. Ghamisi *et al.*, "Advances in Hyperspectral Image and Signal Processing: A Comprehensive Overview of the State of the Art," Dec. 01, 2017, *Institute of Electrical and Electronics Engineers Inc.* doi: 10.1109/MGRS.2017.2762087.

[6] H. Pu, Z. Chen, B. Wang, and G. M. Jiang, "A novel spatial-spectral similarity measure for dimensionality reduction and classification of hyperspectral imagery," *IEEE Transactions on Geoscience and Remote Sensing*, vol. 52, no. 11, pp. 7008–7022, 2014, doi: 10.1109/TGRS.2014.2306687.

[7] C. Rodarmel and J. Shan, "Principal Component Analysis for Hyperspectral Image Classification," *Surveying and Land Information Systems, Vol. 62, No. 2, 2002, pp.115-000*, 2002. [Online].

[8] P. O. Box, L. Van Der Maaten, E. Postma, and J. Van Den Herik, "Tilburg centre for Creative Computing Dimensionality Reduction: A Comparative Review Dimensionality Reduction: A Comparative Review," 2009. [Online]. Available: http://www.uvt.nl/ticc

[9] J. A. Lee and M. Verleysen, *Nonlinear Dimensionality Reduction*. Berlin, Germany: Springer-Verlag, 2007.

[10] H. Huang, G. Shi, H. He, Y. Duan, and F. Luo, "Dimensionality Reduction of Hyperspectral Imagery Based on Spatial-Spectral Manifold Learning," *IEEE Trans Cybern*, vol. 50, no. 6, pp. 2604–2616, Jun. 2020, doi: 10.1109/TCYB.2019.2905793.

[11] Q. Shenming, L. Xiang, and G. Zhihua, "A new hyperspectral image classification method based on spatial-spectral features," *Sci Rep*, vol. 12, no. 1, Dec. 2022, doi: 10.1038/s41598-022-05422-5.

[12] Y. J. Deng, H. C. Li, X. Song, Y. J. Sun, X. R. Zhang, and Q. Du, "Patch Tensor-Based Multigraph Embedding Framework for Dimensionality Reduction of Hyperspectral Images," *IEEE Transactions on Geoscience and Remote Sensing*, vol. 58, no. 3, pp. 1630–1643, Mar. 2020, doi: 10.1109/TGRS.2019.2947200.

[13] A. M. Martõ Ânez and A. C. Kak, "PCA versus LDA," *IEEE Transactions on Pattern Analysis and Machine Intelligence*, Vol. 23, No. 2, Feb. 2001

[14] M Graña, MA Veganzons, B Ayerdi, "Hyperspectral Remote Sensing Scenes," *De Grupo de Inteligencia Computacional (GIC)*. [Online]. Available: http://www.ehu.es/ccwintco/index.php/Sensores-hiperespectrales

[15] A. Ma, A. M. Filippi, Z. Wang, and Z. Yin, "Hyperspectral image classification using similarity measurements-based deep recurrent neural networks," *Remote Sens (Basel)*, vol. 11, no. 2, Jan. 2019, doi: 10.3390/rs11020194.

[16] W. Lv and X. Wang, "Overview of Hyperspectral Image Classification," 2020, *Hindawi Limited*. doi: 10.1155/2020/4817234.

[17] Mayur Vijaykumar Tiwari, "Object Detection in Satellite Images with Canis Hunt Optimized Tetralet Attention enabled Explainable Convolutional Neural Network", *Int J Intell Syst Appl Eng*, vol. 12, no. 4, pp. 45–58, Jun. 2024.